Pulsed EPR Studies of the Semiquinone State of Copper-Containing Amine Oxidases

John McCracken,*,† Jack Peisach,‡ Cheryl E. Cote,§ Michele A. McGuirl,§ and David M. Dooley*,§

Contribution from the Department of Chemistry, Michigan State University, East Lansing, Michigan 48824, Department of Molecular Pharmacology, Albert Einstein College of Medicine, Bronx, New York 10461, and Department of Chemistry, Amherst College, Amherst, Massachusetts 01002. *Received September 6, 1991*

Abstract: The electron spin echo envelope modulation (ESEEM) technique of pulsed EPR spectroscopy was used to further characterize the radical intermediates observed for porcine kidney diamine oxidase and *Arthrobacter* P1 methylamine oxidase when the enzymes were reduced with substrates in the presence of cyanide under anaerobic conditions. The data obtained show that the trapped radical intermediate states found for both enzymes are closely similar. ESEEM studies provide evidence that at least one nitrogen nucleus is magnetically coupled to the paramagnet. Isotopic substitution experiments using [^{14}N]- and [^{15}N]methylamine with *Arthrobacter* P1 methylamine oxidase establish that this coupled nitrogen nucleus is derived from substrate. Stimulated echo ESEEM data collected at X-band for [^{14}N]methylamine with enzyme in the presence of cyanide gives rise to a broad peak in the Fourier transform centered at 3.3 MHz. When [^{15}N]methylamine was used, this spectral component was no longer observed. For porcine kidney diamine oxidase treated with [1,5-$^{14}N_2$]diaminopentane, a similar spectrum with broad features centered at 1.2 and 3.0 MHz was found. Computer simulation of ^{14}N ESEEM data show that such results are expected when large anisotropic hyperfine interactions dominate the electron–nucleus coupling and a perpendicular "edge", in at least one of the powder pattern line shapes, occurs at low frequency. These experiments rule out the possibility that tyrosine or cyanide radicals are responsible for the radical ESR signals observed for substrate-reduced amine oxidase–cyanide complexes and support a mechanism entailing the binding of the amine substrate to the covalently linked quinone cofactor found in both enzymes.

Introduction

Copper-containing amine oxidases are now known to contain an additional covalently bound quinone cofactor,[1-3] recently identified as 6-hydroxydopaquinone.[4] Amine substrates react with the enzyme and undergo a two-electron oxidation to form aldehydes, generating reduced quinone; subsequently, the reduced quinone is reoxidized by molecular oxygen in a copper-dependent process.[1,2,5] A $g = 2$ radical species can be generated by reacting the appropriate amine substrate with various amine oxidases i.e., diamine oxidases from plants[5] and porcine kidney[6] and methylamine oxidase from *Arthrobacter* P1[7] under anaerobic conditions in the presence of cyanide.[5-7] We have previously suggested that this species is a semiquinone radical produced by intramolecular electron transfer from the reduced quinone to Cu(II), thereby generating Cu(I).[6,7] Cyanide is proposed to stabilize Cu(I), shifting the redox partition to favor semiquinone formation.[6,7] This proposal is supported by experiments carried out with methylamine oxidase where the same radical can be observed using *tert*-butyl isocyanide in place of cyanide.[7] Recent EPR studies have established that the Cu(I)–semiquinone state can be generated at ambient temperatures in the absence of cyanide.[8] These results suggest that copper may function as a redox catalyst, mediating electron transfer between the reduced quinone and molecular oxygen, as suggested previously.[9]

When *Arthrobacter* P1 methylamine oxidase was treated anaerobically in the presence of cyanide with [^{15}N]methylamine, a change in EPR line shape of the $g = 2$ signal was observed.[7] This observation indicates that the unpaired electron spin is partially delocalized onto the substrate-derived nitrogen atom. To further characterize this radical intermediate, we have extended this previous continuous-wave EPR study using the electron spin echo envelope modulation technique (ESEEM) of pulsed EPR spectroscopy. Data collected for the *Arthrobacter* and porcine kidney enzymes demonstrate that similar radicals are generated in both systems. Nitrogen modulations in the ESEEM pattern of the methylamine oxidase radical arise from the substrate amine, which is consistent with its formulation as an iminosemiquinone. Parallel studies on porcine kidney amine oxidase, where the $g = 2$ signal is generated using a different amine substrate, show a similar magnetic coupling between the unpaired electron spin and a nitrogen atom.

Materials and Methods

Porcine kidney diamine oxidase and *Arthrobacter* P1 methylamine oxidase were purified, as described previously.[10,11] A detailed description of the procedure used to generate the radical intermediate has been reported.[7] Samples for pulsed EPR spectroscopy were concentrated by ultrafiltration to approximately 0.25–0.5 mM protein (~0.5 – 1.0 mM Cu) in 0.1 M potassium phosphate buffer, pH 7.2. [^{15}N]Methylamine hydrochloride was obtained from Cambridge Isotope Laboratories.

The pulsed EPR spectrometer used in these studies is described elsewhere.[12] The microwave cavity system used for ESEEM measurements employed a folded half-wave resonator[13] together with a Gordon coupling arrangement similar to that described by Britt and Klein.[14] ESEEM

† Michigan State University.
‡ Albert Einstein College of Medicine.
§ Amherst College.

(1) Hartmann, C.; Klinman, J. P. *Biofactors* **1988**, *1*, 41–49.
(2) Knowles, P. F.; Yadav, K. D. S. In *Copper Proteins and Copper Enzymes*; Lontie, R., Ed.; CRC Press: Boca Raton, FL, 1984; Vol. 2, pp 103–129.
(3) Klinman, J. P.; Dooley, D. M.; Duine, J. A.; Knowles, P. F.; Mondovi, B.; Villafranca, J. J. *FEBS Lett.* **1991**, *282*, 1–4.
(4) (a) Janes, S. M.; Mu, D.; Wemmer, D.; Smith, A. J.; Kaur, S.; Maltby, D.; Burlingame, A. L.; Klinman, J. P. *Science* **1990**, *248*, 981–987. (b) Brown, D. E.; McGuirl, M. A.; Dooley, D. M.; Janes, S. M.; Mu, D.; Klinman, J. P. *J. Biol. Chem.* **1991**, *266*, 4049–4051.
(5) Finazzi-Agro, A.; Renaldi, A.; Floris, G.; Rotilio, G. *FEBS Lett.* **1984**, *176*, 378–380.
(6) Dooley, D. M.; McGuirl, M. A.; Peisach, J.; McCracken, J. *FEBS Lett.* **1987**, *214*, 274–278.
(7) Dooley, D. M.; McIntire, W. S.; McGuirl, M. A.; Cote, C. E.; Bates, J. L. *J. Am. Chem. Soc.* **1990**, *112*, 2782–2789.
(8) Dooley, D. M.; McGuirl, M. A.; Brown, D. E.; Turowski, P. N.; McIntire, W. S.; Knowles, P. F. *Nature* **1991**, *349*, 262–264.
(9) Mondovi, B. *Adv. Biochem. Psychopharmacol.* **1972**, *5*, 181–183.
(10) Dooley, D. M.; McGuirl, M. A. *Inorg. Chim. Acta* **1986**, 123, 231–236.
(11) McIntire, W. S. *Methods Enzymol.* **1990**, *188*, 227–235.
(12) McCracken, J.; Peisach, J.; Dooley, D. M. *J. Am. Chem. Soc.* **1987**, *109*, 4064–4072.
(13) Lin, C. P.; Bowman, M. K.; Norris, J. R. *J. Magn. Reson.* **1985**, *65*, 369–374.
(14) Britt, R. D.; Klein, M. P. *J. Magn. Reson.* **1987**, *74*, 535–540.

0002-7863/92/1514-3715$03.00/0

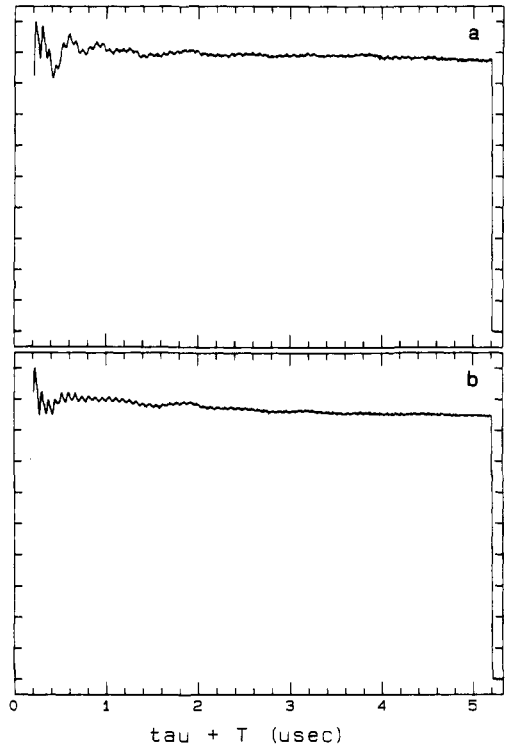

Figure 1. Stimulated echo ESEEM data collected for *Arthrobacter* P1 amine oxidase that was treated anaerobically with (a) [^{14}N]methylamine and (b) [^{15}N]methylamine in the presence of CN^-. Experimental conditions used for these measurements: microwave frequency, 8.88 GHz; magnetic field strength, 3168 G; microwave pulse power, 90 W (15-ns fwhm); τ value, 148 ns; sample temperature, 4.2 K; pulse sequence repetition rate, 10 Hz. Ten events were averaged for each time point. The initial T value (period between second and third microwave pulses) was 52 ns, and 1024 data points were collected at 5-ns intervals.

data were collected using both two-pulse (90°–τ–180°) and three-pulse (90°–τ–90°–T–90°) microwave pulse sequences. Three-pulse data were collected using τ values that ranged from 130 to 400 ns, so that the τ suppression behavior of the resolved modulation frequency components could be examined.[15]

Previous ESEEM studies done on the Cu(II)-binding sites of porcine kidney[12] and *Arthrobacter* P1[16] amine oxidases showed deep ^{14}N modulations likely arising from histidyl imidazole groups strongly bound to the metal. Some residual Cu(II) was present in all samples and contributed to about 10% of the observed electron spin echo amplitude at g = 2.004, where these studies were carried out. Because the spin-lattice relaxation time of the semiquinone species is longer than that of the Cu(II) center, pulse sequence repetition rates were kept below 10 Hz, to ensure maximal contributions from the radical species to the observed echo amplitude. To examine the ESEEM arising from the Cu(I)–semiquinone form of the *Arthrobacter* P1 enzyme free of contributions from the Cu(II) forms, modulation data from samples treated with [^{14}N]methylamine were ratioed with data from samples treated with [^{15}N]methylamine. This procedure was carried out using the protocol described by Mims et al.[17] and proved to be a straightforward means for removing background ^{14}N modulations arising from protein where complete Cu(II) reduction had not occurred. Frequency spectra were obtained by Fourier transformation, using a dead time reconstruction algorithm identical to that described by Mims[18] except that the amplitude correction factors (eq 13 of ref 18) were measured directly from the transformed spectra and entered into an interactive windowing procedure prior to reconstruction.

Computer simulations of ^{14}N ESEEM data were carried out using a procedure outlined previously.[19] Briefly, this approach uses the density matrix formalism developed by Mims[16,20] and applies it to an $S = {}^1/_2$, I = 1 system, where electron–nucleus coupling arises from nuclear

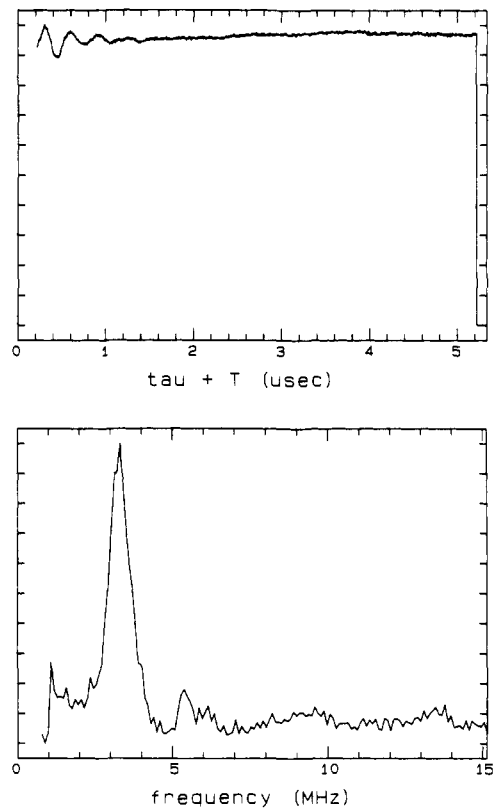

Figure 2. Ratio of the two data sets shown in Figure 1, along with the Fourier transform of the ratio. The [^{14}N]CH_3NH_2 data (Figure 1a) were divided by those obtained using [^{15}N]CH_3NH_2 (Figure 1b).

Zeeman, electron–nuclear hyperfine, and nuclear quadrupole interactions. The procedure considered the electron **g** matrix to be isotropic and calculated ESEEM patterns numerically.[19] Calculations were done on a VAX 11/750 computer, using matrix diagonalization routines from the EISPACK library.[21]

Data collected at different field positions across the g = 2 region provided no evidence for orientation selection effects.[22,23] This result is expected, given the nonselective nature of the microwave pulses employed for ESEEM studies and the small g anisotropy expected for the radical.

Results

Three-pulse (stimulated echo) ESEEM data collected for the *Arthrobacter* P1 enzyme treated anaerobically with [^{14}N]- and [^{15}N]methylamine in the presence of CN^- are shown in Figure 1a,b, respectively. The result of dividing these two data sets to make the background correction mentioned above is given in Figure 2. The Fourier transform of the time domain data that results from this procedure will show its ^{14}N contributions as positive peaks and the corresponding ^{15}N spectral contributions as negative peaks. Examination of Figure 2 shows that the substrate-derived ^{14}N ESEEM spectrum observed for the radical species is dominated by a broad frequency component at 3.3 MHz. There is also a minor ^{14}N component at 5.3 MHz and possibly an additional poorly resolved broad feature at lower frequency. Given the signal-to-noise ratio of the individual measurements and the sensitivity decrease as a result of the division used for obtaining the data shown in Figure 2, one can only be certain about the contribution at 3.3 MHz. However, as we show through spectral simulation (see below), the 5.3-MHz peak is an integral feature of the ^{14}N spectrum.

Results similar to those obtained for *Arthrobacter* P1 amine oxidase were also found for porcine kidney amine oxidase where

(15) Mims, W. B. *Phys. Rev. B: Solid State* **1972**, *5*, 2409–2419.
(16) McCracken, J.; Dooley, D. M.; Peisach, J. Unpublished observations.
(17) Mims, W. B.; Davis, J. L.; Peisach, J. *Biophys. J.* **1984**, *45*, 755–766.
(18) Mims, W. B. *J. Magn. Reson.* **1984**, *59*, 291–306.
(19) Magliozzo, R. S.; McCracken, J.; Peisach, J. *Biochemistry* **1987**, *26*, 7923–7931.
(20) Mims, W. B. *Phys. Rev. B: Solid State* **1972**, *6*, 3543–3545.
(21) Smith, B. T.; Doyle, J. M.; Dongarra, J. J.; Garbow, B. S.; Ikebe, Y.; Klema, V. C.; Moler, C. B. *Matrix Eigensystem Routines—EISPACK Guide*; Springer: New York, 1974; pp 19–22.
(22) Hurst, G. C.; Henderson, T. A.; Kreilick, R. W. *J. Am. Chem. Soc.* **1985**, *107*, 7294–7299.
(23) Hoffman, B. M.; Martinsen, J.; Venters, R. A. *J. Magn. Reson.* **1984**, *59*, 110–123.

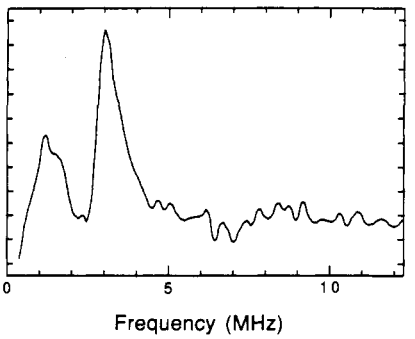

Figure 3. Stimulated echo ESEEM spectrum taken for porcine kidney amine oxidase. Experimental conditions: microwave frequency, 10.097 GHz; field strength, 3596 G; pulse power, 90 W; repetition rate, 10 Hz; τ value, 130 ns; sample temperature, 4.2 K.

the enzyme was treated with 1,5-diaminopentane in the presence of CN^- under anaerobic conditions. Broad peaks centered at 2.8 and 1.2 MHz were observed in the ESEEM spectrum collected at 3005 G, using a microwave frequency of 8.43 GHz. When this sample was studied at a higher magnetic field strength, 3596 G (microwave frequency = 10.1 GHz), the larger broad component moved from 2.8 to 3.0 MHz (Figure 3). The 0.2-MHz shift in frequency is equal to the expected change in the ^{14}N Larmor frequency for a 600 G magnetic field increase. The results of Figures 1–3 show that the nitrogen modulation observed for the radical signal of *Arthrobacter* P1 amine oxidase is substrate derived and that a similar intermediate is also observed for the porcine kidney enzyme.

Absent from the data of Figure 2 are modulation components arising from coupled [^{15}N]methylamine. Such components would give rise to "negative" peaks in the Fourier transform and were not observed for any of the ratioed ESEEM data collected for the *Arthrobacter* enzyme. Precedence for similar observations can be found in the recent literature. ESEEM studies of (dioxygen)cobalt(II) tetraphenylporphyrin (TPP) complexes, with pyridine axially coordinated to the cobalt, gave rise to deep ^{14}N ESEEM arising from magnetic coupling between the pyridine nitrogen and the spin-coupled $(O_2)Co^{II}(TPP)$. When [^{15}N]-pyridine was used to prepare this complex, spectral contributions from coordinated ^{15}N were not observed.[19] Analysis of the ^{14}N ESEEM was carried out, using the density matrix formalism of Mims,[16,20] and showed that the Fermi contact interaction for the axially coordinated ^{14}N was 3.5 MHz, with the anisotropic portion of the tensor being roughly 0.3 MHz. For coordinated [^{14}N]-pyridine, the nuclear quadrupole interaction is comparable to the hyperfine coupling with e^2qQ equal to 2.9 MHz. These authors then scaled the elements of the electron–nucleus hyperfine coupling tensor to the appropriate values for ^{15}N and showed that the expected ESEEM modulation depths for the coupled nucleus would be less than 2% of the spin echo amplitude under the conditions (microwave frequency and magnetic field strength) used to obtain their measurement and would therefore not be resolved. Similar observations have been reported by Eads et al.[24] and DeRose and co-workers.[25] Because ESEEM depths are critically dependent on nuclear-state mixing within an electron spin manifold, observations like those reported in this paper and in the three cited works are not unexpected.

Analysis

Computer simulations of the ^{14}N ESEEM spectra obtained in this study were undertaken to determine how our observations might fit with the proposed model for amine binding to the organic cofactor in these systems[4] and, in general, with the range of hyperfine coupling parameters that give rise to ESEEM like that shown in Figure 2. Because spectra of this type have been observed

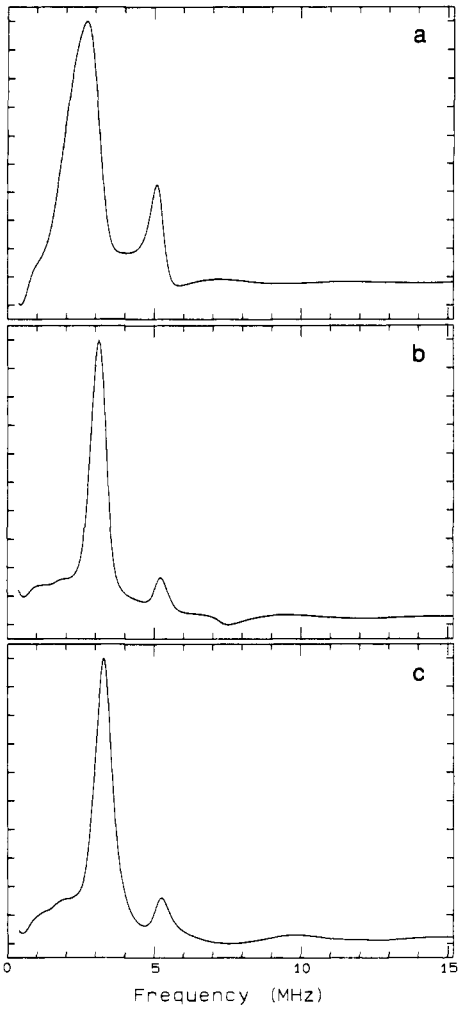

Figure 4. Fourier transforms of three-pulse stimulated echo ESEEM simulations for a single coupled ^{14}N nucleus where $A_\perp$ was fixed at −3.1 MHz and $A_\parallel$ was varied from 6.2 MHz (a) to 12.2 MHz (b) and 24.2 MHz (c). Parameters common to all these simulations: g_n, 0.403 49; magnetic field strength, 3168 G; τ value, 148 ns; e^2qQ, 1.5 MHz; asymmetry parameter 0.4. Electron–nuclear hyperfine and nuclear quadrupole tensors were considered coaxial.

in other systems,[25] it is desirable to know what information can be learned from ^{14}N ESEEM data where only a single well-resolved spectral feature is found. In addition to the requirement that simulations give rise to spectra with a dominant single peak at 3.3 MHz, four other criteria were used to judge the merit of a given calculation. These conditions were as follows: the modulation depths or amplitudes must be less than 10% of the maximum recorded echo amplitude; the resolved frequency component should show the proper shift in frequency when the magnetic field is changed; the amplitude of this resolved frequency component must show the same τ suppression behavior[19,20] for stimulated echo measurements as observed experimentally; and the predicted ^{15}N ESEEM spectra, using hyperfine coupling values that are scaled from those determined for ^{14}N, should show amplitudes that are below the noise level of our measurements. An additional criterion that had to be met by our simulation results was that the ^{14}N couplings should be large enough so that isotopic substitution of the nitrogen would give rise to observable changes in the CW-EPR spectra of the radical intermediate as seen for the *Arthrobacter* P1 enzyme (see Figure 7 of ref 7).

ESEEM simulations where the above criteria were satisfied could only be obtained if the anisotropic part of the electron–nuclear hyperfine coupling was comparable to the isotropic portion and if these couplings were made large in comparison to values that one normally encounters using ESEEM. Specifically, if one considers the ^{14}N hyperfine tensor to be axial and sets $A_\perp = -3.1$

(24) Eads, C. D.; LoBrutto, R.; Kumar, A.; Villaffranca, J. J. *Biochemistry* **1988**, *27*, 165–170.
(25) DeRose, V. J.; Yachandra, V. K.; McDermott, A. E.; Britt, R. D.; Sauer, K.; Klein, M. P. *Biochemistry* **1991**, *30*, 1335–1341.

MHz, $A_\parallel$ values that range from 14 to 24 MHz predict ^{14}N-stimulated echo ESEEM spectra consistent with our experimental results. Figure 4 shows ESEEM spectra simulated using experimental parameters identical to those of Figure 2, where $A_\perp$ for the coupled nitrogen was fixed at −3.1 MHz and $A_\parallel$ varied from 6.2 MHz (Figure 4a) to 24 MHz (Figure 4c). The simulation in Figure 4a shows a broad peak at 2.6 MHz and a sharper frequency component at 5.1 MHz. The modulations obtained for this case, where the hyperfine coupling is completely dipolar, were greater than 50% of the maximum observed spin echo amplitude, ~5 times larger than those observed experimentally. For Figure 4b, $A_\parallel$ was set to 12.2 MHz, and an ESEEM spectrum with a single well-resolved peak at 3.1 MHz and a more minor component at 5.2 MHz was predicted. Although this spectrum is similar to that shown in Figure 2, the predicted modulation depths are still greater than 30%, outside the acceptable range. Figure 4c shows the Fourier transform of simulated ESEEM data obtained when $A_\parallel$ was set to 24 MHz. This spectrum shows a single dominant peak at 3.3 MHz, a minor component at 5.2 MHz, and an overall ESEEM modulation depth of 10%.

Two different coupling ranges gave satisfactory simulations for the data shown in Figure 2. If $A_\perp$ was taken as negative, then the simulation of Figure 4c, where $A_\perp$ = −3.1 MHz and $A_\perp$ = 24 MHz, agrees well with the experimental data. For $A_\perp$ = +3.1 MHz, in $A_\parallel$ of 18 MHz predicted a similar ESEEM spectrum with the appropriate modulation depth. If one considers this axial hyperfine tensor to have the form $A_\perp = A_0^0 - A_2^0$ and $A_\parallel = A_0^0 + 2A_2^0$, then where $A_\perp$ = −3.1 MHz, A_0^0 = 6 MHz and A_2^0 = 9 MHz. For the case where $A_\perp$ is positive, A_0^0 = 8 MHz and A_2^0 = 5 MHz. Although these two parameter sets give good simulations of the data shown in Figure 2, only the parameter set for which $A_2^0 > A_0^0$ predicts the observed τ suppression effects[16,20] for this system. Experiments on the *Arthrobacter* enzyme showed that, in going from the case where τ = 148 ns (Figure 2) to a case where τ = 220 ns, the amplitude of the 3.3 MHz component was greatly reduced. For the $A_0^0 > A_2^0$ case discussed above, changing τ had little effect on the predicted ESEEM amplitude, while, for the $A_2^0 > A_0^0$ case, a 50% reduction in modulation depths is predicted when τ is changed from 148 to 220 ns.

The position of the dominant peak at 3.3 MHz was found to be mostly sensitive to the value of $A_\perp$. Figure 5a shows that, when $A_\perp$ was set to −2.1 MHz with $A_\parallel$ = 24 MHz, using the same nuclear quadrupole coupling constant as in Figure 4, the position of the major peak shifts to 2.7 MHz, similar to ESEEM results obtained from the porcine kidney enzyme (Figure 3). If $A_\perp$ is decreased to −4.1 MHz and the other parameters are fixed as in Figure 4c, the frequency of the dominant spectral feature increases to 3.8 MHz (Figure 5b). Also sensitive to the value of $A_\perp$ is the frequency of the minor component observed at 5.3 MHz for the *Arthrobacter* enzyme (Figure 2). The simulations of Figure 5 show that this spectral feature moves from 4.3 to 6.3 MHz as $A_\perp$ is varied from −2.1 MHz (Figure 5a) to −4.1 MHz (Figure 5b).

With respect to the nuclear quadrupole interaction (nqi), the best simulations were obtained with the nuclear quadrupole coupling constant, e^2qQ, set to values below 2.0 MHz. For larger values of e^2qQ, the spectral feature at 5.3 MHz becomes large and cannot be reduced by rotating the nqi tensor with respect to the hyperfine tensor. Apparently, increasing the size of the nqi alters the nuclear-state mixing within the electron spin manifolds sufficiently to prevent one from obtaining "single"-component spectra like those observed for this system. For the simulations shown in Figures 4 and 5, the nqi and hyperfine tensors were considered coaxial. If the nqi tensor is rotated so that its principal axis is no longer aligned with that of the hyperfine tensor, additional peaks at frequencies above and below 3.3 MHz are predicted.

When the ^{14}N magnetic coupling parameters used for the simulation of Figure 4c are scaled to their appropriate ^{15}N values, $A_\perp$ = −4.3 MHz and $A_\parallel$ = 33.7 MHz, the overall predicted ESEEM depth for a stimulated echo measurement using the experimental conditions (timing parameters) of Figures 1 and 2 is less than 4%. Given that this amplitude will be diminished as a result of background decay arising from spin relaxation processes and that the measurement signal-to-noise ratio will be reduced by the correction procedure, it would be difficult to detect the predicted ^{15}N modulation components at 1.0 and 4.0 MHz. If these ^{15}N hyperfine coupling parameters are used to simulate a two-pulse ESEEM pattern, a single peak at 3.7 MHz is obtained. The predicted modulation depth, in the absence of background decay, is 10%. A weak component at 3.6 MHz was observed in the two-pulse ESEEM data collected for the [^{15}N]methylamine sample in agreement with this prediction, but interference from ^{14}N modulation, arising from residual ESEEM due to the Cu(II) site, prevented further characterization.

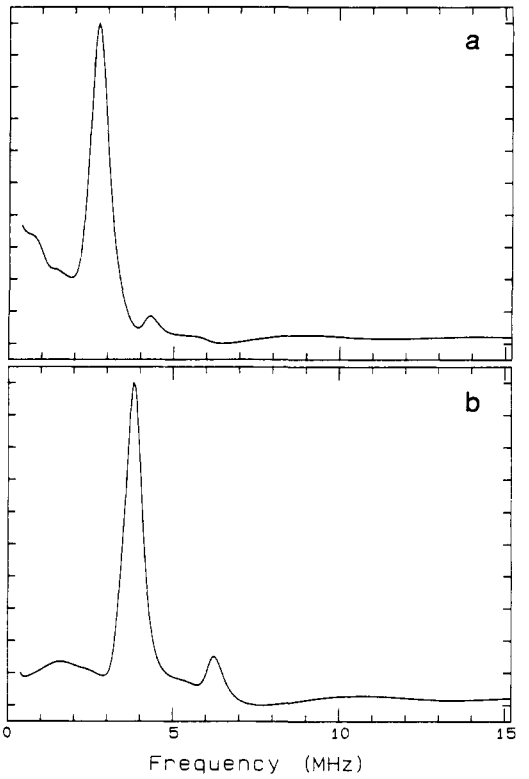

Figure 5. Fourier transforms of three-pulse ESEEM simulations for a single ^{14}N nucleus where $A_\perp$ was −2.1 MHz (a) and −4.1 MHz (b). All other simulation parameters were identical to those of Figure 4c.

Discussion

Most of the ESEEM spectra for ^{14}N reported previously fall into three categories, or coupling ranges, that are much different from those reported here. These categories have been thoroughly treated in the model calculation studies of Reijerse and Keijzers[26] and by Flanagan and Singel[27] and apply to cases where the anisotropic portion of the electron–nuclear hyperfine coupling is small (<20%) with respect to the isotropic or Fermi contact term. A convenient classification scheme is that used by Cosgrove and Singel,[28] which separates ^{14}N ESEEM spectra into groups based on the relative values of $|\nu_n - A_0^0/2|$ and $2K/3$, where ν_n is the Larmor frequency of the coupled ^{14}N nucleus, A_0^0 is the secular portion of the hyperfine coupling tensor, and $K = e^2qQ/4$ is the nuclear quadrupole coupling parameter. The best known spectral type arises when $\nu_n = A_0^0/2$ and is termed the condition of "exact cancellation".[27,29] Typically, the spectra obtained under this condition consist of three sharp, low-frequency lines, which arise from an electron spin manifold where nuclear Zeeman and hyperfine terms cancel, and a broader feature at higher frequency (4–6 MHz). For this case, the echo modulations are deep, often >50% of the maximum amplitude observed.[30,31] ^{14}N ESEEM

(26) Reijerse, E. J.; Keijzers, C. P. *J. Magn. Reson.* **1987**, *71*, 83–96.
(27) Flanagan, H. L.; Singel, D. J. *J. Chem. Phys.* **1987**, *87*, 5606–5616.
(28) Cosgrove, S. A.; Singel, D. J. *J. Phys. Chem.* **1990**, *94*, 8393–8396.
(29) Mims, W. B.; Peisach, J. *J. Chem. Phys.* **1978**, *69*, 4921–4930.

spectra observed when $|\nu_n - A_0^0/2| < 2K/3$ are similar in appearance to those observed for exact cancellation in that one generally resolves four frequency components. This situation has been observed for peptide nitrogens that are hydrogen-bound to Fe–S clusters in two Fe ferredoxins,[32-34] for pyridine bound axially to copper(II) benzoylacetonate,[35] and in a more recent study of the *m*-dinitrobenzene radical absorbed on alumina.[28] For these cases, the ESEEM is weak and superhyperfine couplings are dominated by ^{14}N nuclear quadrupole interactions. For cases where $|\nu_n - A_0^0/2| > 2K/3$, typical ^{14}N ESEEM spectra consist of just two broad peaks corresponding to the "$\Delta m_I = 2$" transitions from each electron spin manifold. This case has been treated by Ashtashkin et al.[36] and reported most often when the isotropic portion of the hyperfine coupling tensor is large. It should also be noted that this type of spectrum can be observed when ν_n dominates the superhyperfine coupling. In the above-mentioned study of the *m*-dinitrobenzene radical,[28] multifrequency ESEEM experiments were used to adjust the value of $|\nu_n - A_0^0/2|$ and convert "two-line" spectra that fall into this third category to ones that consisted of four lines and fall into the second category.

The ^{14}N ESEEM observed in these studies differs from that described by these three cases in that the superhyperfine splittings are dominated by electron–nuclear hyperfine coupling where both isotropic and anisotropic contributions are large. The data and simulations presented above show that under these conditions only the perpendicular singularities of the powder line shapes are resolved. The remaining spectral features are so broad that they are severely damped during the instrument's dead time. For the specific case of the radical found for the *Arthrobacter* enzyme, the broad peak at 3.3 MHz arises from the perpendicular "edge" of the powder pattern line shape due to a "$\Delta m_I = 1$" transition. The field dependence of the frequency of this component assigns it to the electron spin manifold where hyperfine and Zeeman terms are additive. This point is best illustrated by the frequency histograms shown in Figure 6. These histograms are generated using a method described by Mims[29] and represent all possible superhyperfine frequencies that could arise for a given set of coupling constants weighted by $\sin\theta$, where θ is the angle between the principal axes of the hyperfine coupling tensor and the laboratory magnetic field. No weightings for nuclear-state mixing or constraints imposed by spectrometer dead time are included in the calculation. Figure 6a shows a complete histogram for the three nuclear transitions possible for both electron spin manifolds, which was determined by using the spin Hamiltonian parameters of Figure 4c. Peaks at 1.0, 3.2, and 5.3 MHz are found superimposed on a broad spectrum that covers the range from 0 to 20 MHz. Parts b and c of Figure 6 show powder line shapes due to just the "$\Delta m_I = 1$" transitions from the $m_S = +^1/_2$ and $-^1/_2$ manifolds, respectively. The minor peak at 5.3 MHz arises from the "$\Delta m_I = 2$" transition of the $m_S = ^1/_2$ manifold.

Both standard X-band EPR spectra[7] and, more importantly, the ESEEM modulation patterns obtained in this study (Figures 1–3) are consistent with the presence of similar radicals in porcine kidney diamine oxidase and *Arthrobacter* P1 methylamine oxidase, following anaerobic reduction by amine substrates in the presence of cyanide. This conclusion is in accord with previous spectroscopic comparisons.[6-8] Recent work has shown that this radical can be generated at room temperature in the absence of cyanide. Collectively, the data also establish that similar reduced-enzyme

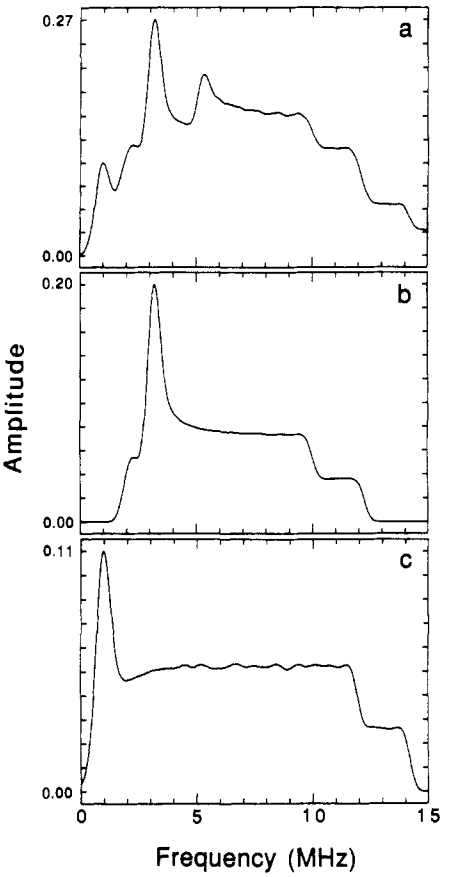

Figure 6. "Frequency histograms" of ^{14}N superhyperfine splittings calculated for a single ^{14}N nucleus coupled to an electron spin using spin Hamiltonian parameters identical to those of Figure 4c. The amplitudes of the computed superhyperfine frequencies were given a $\sin\theta$ weighting, where θ represents the angle between the principal axis of the electron–nucleus hyperfine coupling tensor and the laboratory magnetic field. For (a), contributions from both $\Delta m_I = 1$ and $\Delta m_I = 2$ transitions of both electron spin manifolds are plotted. For (b), only $\Delta m_I = 1$ contributions from the $m_S = +^1/_2$ manifold are shown, while the pattern for (c) consists only of $\Delta m_I = 1$ contributions from the $m_S = -^1/_2$ manifold. The integration over all possible orientations of the laboratory field, with respect to the hyperfine tensor principal axes, was divided into 1° increments. Each "stick" in the powder pattern was convoluted with a Gaussian line shape of 0.3-MHz fwhm to obtain the powder patterns shown in the figure.

radicals can be generated in copper-containing amine oxidases from bacterial, plant, and mammalian sources. Since different enzymes and substrates are involved, the radical must be associated with an amino acid (e.g., tyrosine or tryptophan) or the quinone cofactor.

The magnetic coupling parameters obtained for substrate-derived ^{14}N are consistent with previous formulations of this radical species as arising from an iminosemiquinone. The values for A_0^0 and A_2^0 for the hyperfine coupling tensor, 6 and 9 MHz, respectively, are in line with what one would expect for a π-radical where covalent attachment of the substrate amine nitrogen to an aromatic residue or cofactor has occurred. A nitrogen isotropic hyperfine coupling constant of 6 MHz falls in the range of values reported for *o*- and *p*-dinitrobenzene radical anions.[37,38] Also, if the unpaired electron spin density is confined to the π molecular orbitals of such an intermediate, the hyperfine coupling would be expected to have a large anisotropic contribution. A decrease in the nuclear quadrupole coupling constant, e^2qQ, from a value of 4.0 MHz, as found for methylamine,[39] to less than 2.0 MHz indicates that the amine nitrogen has lost much of its lone-pair

(30) Jiang, F.; McCracken, J.; Peisach, J. *J. Am. Chem. Soc.* **1990**, *112*, 9035–9044.
(31) Goldfarb, D.; Fauth, J.-M.; Tor, Y.; Shanzer, A. *J. Am. Chem. Soc.* **1991**, *113*, 1941–1948.
(32) LoBrutto, R.; Haley, P. E.; Yu, C. A.; Ohnishi, T.; Leigh, J. S. *Biophys. J.* **1986**, *49*, 327a.
(33) Thomann, H.; Morgan, T. V.; Jin, H.; Burgmayer, S. J. N.; Bare, R. E.; Stiefel, E. I. *J. Am. Chem. Soc.* **1987**, *109*, 7913–7914.
(34) Cammack, R.; Chapman, A.; McCracken, J.; Cornelius, J. B.; Peisach, J.; Weiner, J. H. *Biochim. Biophys. Acta* **1988**, *956*, 307–312.
(35) Cornelius, J. B.; McCracken, J.; Clarkson, R. B.; Belford, R. L.; Peisach, J. *J. Phys. Chem.* **1990**, *94*, 6977–6982.
(36) Ashtashkin, A. V.; Dikanov, S. A.; Tsvetkov, Yu. D. *J. Struct. Chem. (Engl. Transl.)* **1984**, *25*, 45–55.
(37) Freed, J. H.; Fraenkel, G. K. *J. Chem. Phys.* **1964**, *40*, 1815–1829.
(38) Maki, A. H.; Geske, D. H. *J. Chem. Phys.* **1960**, *33*, 825–832.
(39) Lucken, E. A. C. *Nuclear Quadrupole Coupling Constants*; Academic Press: New York, 1969; pp 217–248.

character in its conversion to an imine.

Tyrosine radicals have now been identified in several proteins or enzymes.[40-43] However, the results reported herein, together with additional recent results, effectively rule out this possibility for the radical observed in substrate-reduced amine oxidases. First, a significant $^{14}N/^{15}N$ isotope effect on the X-band EPR spectrum of the *Arthrobacter* methylamine oxidase has been previously observed.[7] The results shown in Figure 2 establish that this arises from coupling between the nitrogen nucleus of the substrate amine and the unpaired electron. Second, this coupling is reasonably strong, as indicated by the hyperfine coupling constants obtained from the ^{14}N ESEEM simulations and the even-larger value inferred for ^{15}N (see above). It is, therefore, highly unlikely that the observed nitrogen modulations are due to nonbonded atoms. Since we are aware of no chemically plausible mechanism by which the nitrogen from the substrate amine can be incorporated into a tyrosine residue under physiological conditions, we conclude that a tyrosine radical (or a radical derived from any other amino acid) is not the source of the EPR in substrate-reduced amine oxidases.

The presence of the substrate amine nitrogen in substrate-reduced amine oxidases is consistent with previous mechanistic suggestions[1,2,4,44,45] and with the reactivity expected of a quinone-like cofactor.[3,46,47] These results are also consistent with our previous proposal[7,8] that internal electron transfer from the reduced quinone to Cu(II) is the mechanism by which the semiquinone state of amine oxidases may be generated.

Acknowledgment. We thank Dr. William McIntire for several helpful discussions. This research was supported by National Institutes of Health Grants GM 27659 to D.M.D., RR02583 and GM 40168 to J.P., and GM 45795 to J.M.

Registry No. Diamine oxidase, 9001-53-0; methylamine oxidase, 80891-30-1.

(40) Sjoberg, B. M.; Reichard, P.; Gräslund, A.; Ehrenberg, A. *J. Biol. Chem.* **1978**, *253*, 6863-6865.
(41) Stubbe, J. *Biochemistry* **1988**, *27*, 3893-3900.
(42) Barry, B. A.; Babcock, G. T. *Proc. Natl. Acad. Sci. U.S.A.* **1987**, *84*, 7099-7103.
(43) Whittaker, M. M.; Whittaker, J. W. *J. Biol. Chem.* **1990**, *265*, 9610-9613.
(44) Rius, F. X.; Knowles, P. F.; Pettersen, G. *Biochem. J.* **1984**, *220*, 767-772.
(45) Bellelli, A.; Brunori, M.; Finazzi-Ogro, A.; Flous, G.; Giartosi, A.; Rinaldi, A. *Biochem. J.* **1985**, *232*, 923-926.
(46) Hartmann, C.; Klinman, J. P. *FEBS Lett.* **1990**, *261*, 441-444.
(47) Sleath, P. R.; Noar, J. B.; Eberlein, G. A.; Bruice, T. C. *J. Am. Chem. Soc.* **1985**, *107*, 3328-3338.

Evaluation of Mn(II) Framework Substitution in MnAPO-11 and Mn-Impregnated $AlPO_4$-11 Molecular Sieves by Electron Spin Resonance and Electron Spin-Echo Modulation Spectroscopy

Guillaume Brouet, Xinhua Chen, Chul Wee Lee, and Larry Kevan*

Contribution from the Department of Chemistry, University of Houston, Houston, Texas 77204-5641. *Received September 9, 1991*

Abstract: MnAPO-11 and Mn-impregnated $AlPO_4$-11 (Mn-$AlPO_4$-11) samples were prepared with various manganese contents and studied by electron spin resonance (ESR) and electron spin-echo modulation (ESEM). At high manganese content (4.25 mol %), the spin-spin interaction broadens the ESR spectra of MnAPO-11 and Mn-$AlPO_4$-11 so that they show only a broad line at $g = 2.01$. At low manganese content (0.1 mol %), the ESR spectra of MnAPO-11 and Mn-$AlPO_4$-11 exhibit the same parameters ($g = 2.01$ and $A \approx 93.5$ G), but the spectra obtained from MnAPO-11 samples are better resolved. Two-pulse ESEM of MnAPO-11 and Mn-$AlPO_4$-11 with adsorbed deuterium oxide shows that the local environments of manganese in the hydrated samples are different. This indicates that the manganese species environments in MnAPO-11 and Mn-$AlPO_4$-11 are different, suggesting that Mn(II) is framework substituted in MnAPO-11 since it obviously occupies an extra-framework position in Mn-$AlPO_4$-11. The framework incorporation in MnAPO-11 is confirmed by a three-pulse ESEM study of deuterium modulation resulting from interactions of deuterated adsorbates with manganese which indicate that the manganese occupies a negatively charged site in MnAPO-11.

Introduction

A new class of microporous aluminophosphate molecular sieves ($AlPO_4$) has been described.[1] Some of these materials are structurally similar to zeolites while others, like $AlPO_4$-5 and $AlPO_4$-11, have novel three-dimensional framework structures. The replacement of elements that constitute the framework of these molecular sieves has been studied for various $AlPO_4$ structures.[2] This is of particular interest since these materials do not show any Brønsted acidity due to their neutral framework resulting from an Al/P ratio of 1. Incorporation of silicon for mostly phosphorus gives silicoaluminophosphates (SAPO) which are structurally analogous to the $AlPO_4$ series.[3] Some transition metal ions can also be incorporated which is of particular interest since various transition metal species are involved in catalytic processes.

The framework substitution of divalent manganese for some Al(III) in $AlPO_4$-11, denoted MnAPO-11, has been reported.[2,4] Indirect evidence for framework incorporation of Mn(II) in MnAPO-11 includes chemical analysis and measurement of Brønsted acidity. Some chemical analyses of MnAPO-11 showed that it contained less aluminum than phosphorus, which is expected if manganese actually replaces aluminum within the framework

(1) Wilson, S. T.; Lok, B. M.; Messina, C. A.; Cannan, T. R.; Flanigen, E. M. *J. Am. Chem. Soc.* **1982**, *104*, 1146.
(2) Flanigen, E. M.; Lok, B. M.; Patton, R. L.; Wilson, S. T. In *New Developments in Zeolite Science and Technology*; Murakami, Y., Iijima, A., Ward, J. W., Eds.; Elsevier: Amsterdam, 1986; pp 103-112.
(3) Lok, B. M.; Messina, C. A.; Patton, R. L.; Gajek, R. T.; Cannan, T. R.; Flanigen, E. M. *J. Am. Chem. Soc.* **1984**, *106*, 6092.
(4) Wilson, S. T.; Flanigen, E. M. U.S. Patent 4 567 029, 1985.

0002-7863/92/1514-3720$03.00/0